0026-895X/07/7105-1258–1267$20.00
MOLECULAR PHARMACOLOGY
Vol. 71, No. 5
29108/3201022
Mol Pharmacol 71:1258–1267, 2007
Printed in U.S.A.

Synergistic Neuroprotection by Bis(7)-tacrine via Concurrent Blockade of *N*-Methyl-D-aspartate Receptors and Neuronal Nitric-Oxide Synthase[S]

Wenming Li, Jian Xue, Chunying Niu, Hongjun Fu, Colin S. C. Lam, Jialie Luo, Hugh H. N. Chan, Huaiguo Xue, Kelvin K. W. Kan, Nelson T. K. Lee, Chaoying Li, Yuanping Pang, Mingtao Li, Karl W. K. Tsim, Hualiang Jiang, Kaixian Chen, Xiaoyuan Li, and Yifan Han

Departments of Biochemistry (W.L., H.F., C.S.C.L., J.L., H.H.N.C., K.K.W.K., N.T.K.L., Y.H.), Chemistry (J.X., H.X., X.L.), and Biology (K.W.K.T.), Hong Kong University of Science and Technology, Hong Kong, China; Center for Drug Discovery and Design, State Key Laboratory of Drug Research, Shanghai Institute of Materia Media, Shanghai, China (C.N., H.J., K.C.); Laboratory of Molecular and Cellular Neurobiology, National Institute on Alcohol Abuse and Alcoholism, National Institutes of Health, Bethesda, Maryland (C.L.); Mayo Foundation for Medical Education and Research, Rochester, Minnesota (Y.P.) and Department of Pharmacology and Proteomics Lab, Zhongshan Medical College, Sun Yat-sen University, Guangzhou, China (W.L., M.L.)

Received July 23, 2006; accepted February 13, 2007

ABSTRACT

The excessive activation of the *N*-methyl-D-aspartate receptor (NMDAR)/nitric oxide (NO) pathway has been proposed to be involved in the neuropathology of various neurodegenerative disorders. In this study, NO was found to mediate glutamate-induced excitotoxicity in primary cultured neurons. Compared with the NO synthase (NOS) inhibitor, N^G-monomethyl-L-arginine (L-NMMA), and the NMDAR antagonist memantine, bis(7)-tacrine was found to be more potent in reducing NO-mediated excitotoxicity and the release of NO caused by glutamate. Moreover, like L-NMMA but not like 5*H*-dibenzo[*a*,*d*]cyclohepten-5,10-imine (MK-801) and memantine, bis(7)-tacrine showed greater neuroprotection and inhibition on NO release when neurons were pretreated for a prolonged time between 0 and 24 h and remained quite potent even when neurons were post-treated 1 h after the glutamate challenge. Bis(7)-tacrine was additionally found to be as moderately potent as memantine in competing with [^{3}H]MK-801, inhibiting NMDA-evoked currents and reducing glutamate-triggered calcium influx, which eventually reduced neuronal NOS activity. More importantly, at neuroprotective concentrations, bis(7)-tacrine substantially reversed the overactivation of neuronal NOS caused by glutamate without interfering with the basal activity of NOS. Furthermore, in vitro pattern analysis demonstrated that bis(7)-tacrine competitively inhibited both purified neuronal and inducible NOS with IC_{50} values at 2.9 and 9.3 μM but not endothelial NOS. This result was further supported by molecular docking simulations that showed hydrophobic interactions between bis(7)-tacrine and three NOS isozymes. Taken together, these results strongly suggest that the substantial neuroprotection against glutamate by bis(7)-tacrine might be mediated synergistically through the moderate blockade of NMDAR and selective inhibition of neuronal NOS.

This work was supported by grants from the Research Grants Council of Hong Kong (HKUST 6120/02M, 6133/03M, 6140/02M, and 6441/06M; 643/99; AoE/B15/01; P_10/01); the National Science Foundation of China (30370450, 30170299, and 30570562), and the CPD Foundation (20060390210).

Article, publication date, and citation information can be found at http://molpharm.aspetjournals.org.

doi:10.1124/mol.106.029108.

[S] The online version of this article (available at http://molpharm.aspetjournals.org) contains supplemental material.

The precise mechanisms leading to the pathogenesis of chronic and acute neurodegenerative disorders have not yet been fully elucidated. However, increasing evidence has shown that these diseases may share a final common pathway to neuronal injury as a result of the excitotoxicity caused by the overstimulation of glutamate receptors of the *N*-methyl-D-aspartate (NMDA) subtype (Yuan and Yankner, 2000;

ABBREVIATIONS: NMDA, *N*-methyl-D-aspartate; AChE, acetylcholinesterase; ANOVA, analysis of variance; CGN, cerebellar granule neuron; NOS, nitric-oxide synthase; eNOS, endothelial nitric-oxide synthase; iNOS, inducible nitric-oxide synthase; nNOS, neuronal nitric-oxide synthase; L-NMMA, N^G-monomethyl-L-arginine; MTT, 3(4,5-dimethylthiazol-2-yl)-2,5-diphenyltetrazolium bromide; NMDAR, *N*-methyl-D-aspartate receptor; BAPTA, 1,2-bis(2-aminophenoxy)ethane-*N*,*N*,*N*′,*N*′-tetraacetic acid; DIV, days in vitro; 7-NI, 7-nitroindozale; MK-801, 5*H*-dibenzo[*a*,*d*]cyclohepten-5,10-imine; ARL17477, *N*-[4-(2-[[(3-chlorophenyl)methyl]amino]ethyl)phenyl]-2-thiophenecarboximidamide dihydrochloride; 3D, three-dimensional.

Sonkusare et al., 2005). Excessive nitric oxide (NO), generated by neuronal NO synthase (nNOS), which is tethered to the NMDA receptor (NMDAR) and activated by Ca^{2+} overinflux via the receptor-associated ion channel, mediates the downstream signal transduction of the NMDAR (Yamauchi et al., 1998; Lipton, 2004) and leads to the excitotoxic neuronal cell death (Boje, 2004; Lipton, 2004). Given the role that NMDAR/NO signaling plays during the development and progression of various neurodegenerative diseases, reducing excessive NO generation by directly/indirectly inhibiting nNOS may be an excellent strategy for preventing and treating neurodegenerative disorders (Grunewald and Beal, 1999; Fedorov et al., 2004; Lipton, 2004). Actually, the use of NMDAR antagonists for neurodegenerative diseases has been realized in the use of memantine (a moderate antagonist of NMDAR) in successful treatment of moderate to severe Alzheimer's disease (Sonkusare et al., 2005); additionally, several nNOS inhibitors such as 7-nitroindozale (7-NI) and ARL17477 have been demonstrated as promising candidates for treating other neurodegenerative diseases such as stroke (Lipton, 2004; Willmot et al., 2005).

On the other hand, because multifactorial etiopathogenesis is clearly indicated in neurodegenerative disorders, multiple drug therapy is required to address the varied pathological aspects of these diseases (Mattson, 2004). Current approaches with one-drug-one-target only offer limited and transient benefits to patients but do not significantly delay the course of neurodegeneration (Frantz, 2005; Youdim and Buccafusco, 2005). Multifunctional compounds might provide greater therapeutic efficacy by targeting different sites in the brain concurrently (Zhang, 2005; Van der Schyf et al., 2006). Therefore, new one-drug-multiple-targets approaches have been developed expressly to target multiple sites in the central nervous system with single molecular entities for the treatment of these diseases (Youdim and Buccafusco, 2005; Zhang, 2005).

Over the past few years, we have demonstrated that bis(7)-tacrine, a dimeric acetylcholinesterase (AChE) inhibitor, may be a multifunctional entity with the following properties. In brief, bis(7)-tacrine has been reported as a promising therapeutic agent for Alzheimer's disease on the basis of its AChE inhibition (Pang et al., 1996; Wang et al., 1999) and superior memory-enhancement capabilities (Liu et al., 2000). Moreover, bis(7)-tacrine protects against ischemia-induced injury in mouse astrocytes (Wu et al., 2000) and hydrogen peroxide-induced apoptosis in PC12 cells (Xiao et al., 2000). Recently, we also reported that bis(7)-tacrine prevents glutamate-induced apoptosis in cerebellar granule neurons (CGNs) by blocking NMDAR (Li et al., 2005), and it attenuates NOS/NO-mediated neurotoxicity (Li et al., 2006) and β-amyloid-induced apoptosis in cortical neurons (Fu et al., 2006). It has also been found that although bis(7)-tacrine has a similar affinity and potency to memantine in blocking NMDAR, this dimer is much more potent than memantine in preventing glutamate-induced excitotoxicity in neurons (Li et al., 2005; Sonkusare et al., 2005).

In the present study, the molecular mechanisms underlying the more potent neuroprotection by bis(7)-tacrine are further examined in primary cultured neurons. We demonstrate that the substantial neuroprotection of bis(7)-tacrine may be concurrently mediated through direct and selective inhibition of nNOS and through moderate blockade of NMDAR, which plays a synergistic role in inhibiting endogenous NOS and then reducing NO generation. More importantly, at neuroprotective concentrations, bis(7)-tacrine has almost no interference with the basal activity of NOS in live neurons. The substrate kinetics of NOS inhibition and molecular simulation further indicate that bis(7)-tacrine selectively inhibits the neuronal subtype of NOS in a competitive manner.

Materials and Methods

Primary CGN Cultures. Rat CGNs were prepared from 8-day-old Sprague-Dawley rats as described previously (Li et al., 2005). In brief, neurons were seeded at a density of 2.0×10^6 cells/ml in basal modified Eagle's medium (Invitrogen, Carlsbad, CA) containing 10% fetal bovine serum, 25 mM KCl, 2 mM glutamine, and penicillin (100 U/ml)/streptomycin (100 μg/ml). Cytosine arabinoside (10 μM) was added to the culture medium 24 h after plating to limit the growth of non-neuronal cells. With the use of this protocol, 95 to 99% of the cultured cells were granule neurons.

Measurement of Neurotoxicity. The percentage of surviving neurons was estimated by determining the activity of mitochondrial dehydrogenases with the 3(4,5-dimethylthiazol-2-yl)- 2.5-diphenyltetrazolium bromide (MTT) assay (Li et al., 2005). The assay was performed according to the manufacturer's specifications (MTT Kit I; Roche Applied Science, Indianapolis, IN). In brief, neurons were cultured in 96-well plates; 10 μl of 5 mg/ml MTT-labeling reagent was added to each well in 100 μl of medium, and the plate was incubated for 4 h in a humidified incubator at 37°C. After the incubation, 100 μl of the solvating solution (0.01 N HCl in 10% SDS solution) was added to each well for 18 h. The absorbance of the samples was measured at a wavelength of 570 nm with 630 nm as a reference wavelength. Unless otherwise indicated, the extent of MTT conversion in the cells exposed to glutamate is expressed as a percentage of the control.

NO Release Detecting Assay. All electrochemical assays were performed with an Electrochemical Workstation in a 10-ml small, airtight beaker. For the sensors fabrication and NO measurements, the three-electrode system included an Au wire (Φ, 0.5 mm) as the counter electrode, a modified Ag/AgCl wire (Φ, 0.2 mm) as the reference electrode, and a chemically modified platinum microelectrode (Φ, 50 μm) with a modifier similar to that used in our previous report (Xue et al., 2000). In the electroanalytical experiments, a CHI660A Potentiosat was used with a preamplifier. The calibrated NO sensors were used for the following tests, which were conducted on the stage of an inverted stereomicroscope. The three-electrode system was bound together to ensure the immobile distance between each electrode. Under the stereomicroscope, the bound electrodes were positioned by approximately 10 μm close to the neurons. The data were qualitatively analyzed by differential pulse amperometry techniques.

Confocal Laser Scanning Microscopy. A confocal laser scanning microscope was used to evaluate relative changes in intracellular calcium concentrations ($[Ca^{2+}]_i$) by monitoring the Fluo-3 fluorescence after intracellular cleavage of a superfused Fluo-3 acetoxymethylester (5×10^{-6} M, with excitation at 488 nm and emission at >510 nm) (Li et al., 2005). In brief, neurons were stained with 5×10^{-6} M Fluo-3 acetoxymethylester for 30 min in a 37°C incubator and then washed three times with a balanced salt solution containing 154 mM NaCl, 25 mM KCl, 0.035 mM Na_2HPO_4, 2.3 mM $CaCl_2$, 3.6 mM $NaHCO_3$, 5.6 mM glucose, and 5 mM HEPES, pH 7.4. The fluorescence images were analyzed using the MetaMorph software package (Molecular Devices, Sunnyvale, CA). Data were obtained by evaluating the fluorescence (F) from selected areas within a cell, after subtraction of background fluorescence, and division by the fluorescence intensity before drug application (F_0), expressed as F/F_0. Confocal images were taken and stored every 5 to 10 s. Bis(7)-

tacrine was added to the balanced salt solution 30 min before the addition of glutamate.

Whole-Cell Electrophysiological Analysis. Cultures of hippocampal neurons on glial feeder layers were prepared from 15- to 17-day fetal mice for the whole-cell patch clamp analysis (Li et al., 2005). The hippocampi were dissected in Hanks' buffered salt solution containing 10 mM HEPES, DNase type I (Roche Applied Science), and 1 mM sodium pyruvate, pH 7.4; incubated in 0.25% trypsin (Invitrogen) in Hanks' buffered salt solution at 37°C for 15 min; washed three times in Hanks' buffered salt solution at room temperature; and triturated 30 to 40 times using a fire-polished Pasteur pipet. Neurons were plated on confluent layers of hippocampal glia in minimum essential medium containing 10% heat-inactivated equine serum (HyClone, Logan, UT) and 1 mM sodium pyruvate. After 4 h, half of this medium was replaced with a maintenance medium consisting of minimum essential medium, 1 mM sodium pyruvate, and N2 serum supplement (Invitrogen); this medium was subsequently given half-changes weekly. Neurons were cultured for 2 weeks before use in the experiments.

Whole-cell patch-clamp recording was carried out at room temperature using an EPC-7 patch clamp amplifier (Strijbos et al., 1996; Li et al., 2005). The membrane potential was held at −60 mV. Data were filtered at 2 kHz (8-pole Bessel) and acquired on a computer (5 kHz sampling frequency) during the experiments using a DigiData 1200A interface and pClamp software (Molecular Devices). Neurons were superfused at 1 to 2 ml/min in an extracellular medium containing 150 mM NaCl, 5 mM KCl, 0.2 mM $CaCl_2$, 10 mM HEPES, 10 mM glucose, and 0.0002 mM tetrodotoxin, and the pH was adjusted to 7.4 using NaOH and the osmolality to 340 mOsmol/kg using sucrose. Low Ca^{2+} was maintained to minimize NMDAR inactivation. The recording pipette solution contained 130 mM CsCl, 4 mM Mg_4ATP, 10 mM BAPTA, and 10 mM HEPES, and pH was adjusted to 7.4 using CsOH and osmolality to 310 mOsmol/kg using sucrose. Solutions of agonists and drugs were prepared in extracellular media and were applied to neurons by gravity flow from a linear barrel array consisting of fused silica tubes (internal diameter, ~200 μm) connected to independent reservoirs; solutions were exchanged by shifting the pipette horizontally using a micromanipulator.

Receptor-Ligand Binding Assay. The binding assay was performed and a synaptic plasma membrane was prepared from the cerebella of 15-day-old Sprague-Dawley rats by using discontinuous sucrose density gradients as described previously (Li et al., 2005). The receptor-ligand binding was performed in triplicate using 150 to 200 μg of the synaptic plasma membrane protein and 4 nM [^{3}H]MK-801 (American Radiolabeled Chemicals Inc., St. Louis, MO) incubated with different concentrations of testing compounds; nonspecific binding was determined by an excess of the nonradioactive MK-801. After collecting the samples on Whatman GF/B filters by rapid filtration with a MD-24 Sample Harvester, the filtrated tissue on the filters was soaked into scintillation cocktails overnight and measured in a scintillation counter (1209 Rackbeta; Wallac Oy, Turku, Finland). Specific ^{3}H-ligand binding to receptors was determined by subtracting the nonspecific count from the total, which is defined by 0.1 mM unlabeled MK-801. The K_i values are derived from the IC_{50} values by correcting for receptor occupancy by ^{3}H-ligand. The binding parameters were obtained with the ligand binding module in Sigma Plot 9.0 program (SPSS Inc., Chicago, IL).

NOS Activity Assays. For the NOS activity assay in neurons (Li et al., 2006), the activity of NOS was measured in CGNs by an assay kit (Calbiochem, Darmstadt, Germany). The total levels of nitrate and nitrite were detected for indirectly reflecting NOS activity by following the kit's instructions. Ten microliters of supernatant of CGNs from 96-well plates exposed to 75 μM glutamate for 2 min was transferred into a fluorescent plate and incubated with 10 μl of nitrate reductase and enzyme cofactors for 1 h at room temperature. Afterward, 10 μl of 2,3-diaminonaphthalene was used as the substrate to react with the nitrite for 10 min. After quenching the reaction by adding 2.8 M NaOH, the fluorescent signal of the product, *L*(H)-naphthotriazole, was measured with the excitation of 365 nm and emission of 540 nm. The actual amount of nitrate was determined from the standard curves constructed by the nitrate standard provided.

In the in vitro NOS activity assay, purified recombinant human nNOS, endothelial NOS (eNOS), and inducible NOS (iNOS) were bought from Alexis Biochemicals (Lausen, Switzerland). NOS activity was determined by monitoring the conversion of L-[^{3}H]arginine to [^{3}H]citrulline following the kit's instructions (Calbiochem). The reaction mixture contained a final volume of 40 μl with 25 mM Tris-Cl at pH 7.4, 3 μM tetrahydrobiopterin, 1 μM FAD, 1 μM FMN, 1 mM NADPH, 0.6 mM $CaCl_2$, 0.1 μM calmodulin, 2.5 μg of pure NOS enzyme, 5 μM L-[^{3}H]arginine (GE Healthcare, Chalfont St. Giles, Buckinghamshire, UK), and different concentrations of the tested reagents. The reaction mixture was incubated at 37°C for 30 to 45 min. The reaction was quenched by adding 400 μl of stopping buffer (50 mM HEPES, pH 5.5, and 5 mM EDTA) for nNOS and eNOS reactions or by heating reactive tubes for iNOS. Unreacted L-[^{3}H]arginine was then trapped by 100 μl of provided equilibrated resin in a spin cup followed by centrifugation for 1 min at 10,000 rpm. The filtrate was quantified by liquid scintillation counting.

Molecular Docking Technique. The crystal structures of nNOS, iNOS, and eNOS from the Protein Data Bank (Fischmann et al., 1999; Berman et al., 2000; Fedorov et al., 2004) were used in the docking studies. Ligands and water were removed from the crystal structures of the protein, and hydrogen atoms were then added. The potential 3D structures of nNOS, iNOS, and eNOS were assigned with Consistent Valence ForceField, which was encoded in the molecular modeling software Insight II (Accelrys, Inc., San Diego, CA). The structure of bis(7)-tacrine was generated by Insight II. Automated molecular docking between all molecules was performed by using the advanced docking program AutoDock 3.0.5, whereas the inhibitor-enzyme interactions were estimated by the Lamarckian genetic algorithm. A 3D grid with 52 × 52 × 52 points and a spacing of 0.375 Å was created by the AutoGrid algorithm (Morris et al., 1998) to evaluate the binding energies between proteins and ligands. At this stage, the protein was embedded in the 3D grid, and a probe atom was placed at each grid point. The affinity and electrostatic potential grid were calculated for each type of atom in the ligand. The energetics of a particular inhibitor configuration was found by trilinear interpolation of affinity values and electrostatic interactions of the eight grid points surrounding each of the atoms of the ligand. A series of the docking parameters was set. The atom types and the generations and the number of runs for the Lamarckian genetic algorithm were edited and properly assigned according to the Amber force field requirements. The number of generations, energy evaluations, and docking runs were set to 370,000, 1,500,000, and 120, respectively. The docked complexes of the ligand-enzyme were selected according to the interacting energy combined with the geometrical matching quality.

Data Analysis and Statistics. Data are expressed as mean ± S.E.M., and statistical significance was determined by analysis of variance (ANOVA) with Dunnett's test. Differences were accepted as significant at $p < 0.05$ or less.

Results

NO Mediates Glutamate-Induced Excitotoxicity in Neurons. At 8 days in vitro (DIV), CGNs were exposed to glutamate at concentrations from 0 to 150 μM. The cell viability was detected by MTT assay at 24 h after the glutamate challenge, and the NO release was measured by electrochemical methods from 10 min before to 30 min after the glutamate challenge. As shown in Fig. 1A, glutamate caused NO release and cell death in a concentration-dependent manner. CGNs were pretreated with 10 to 200 μM L-NMMA for 2 h and then exposed to 75 μM glutamate for 24 h. We found

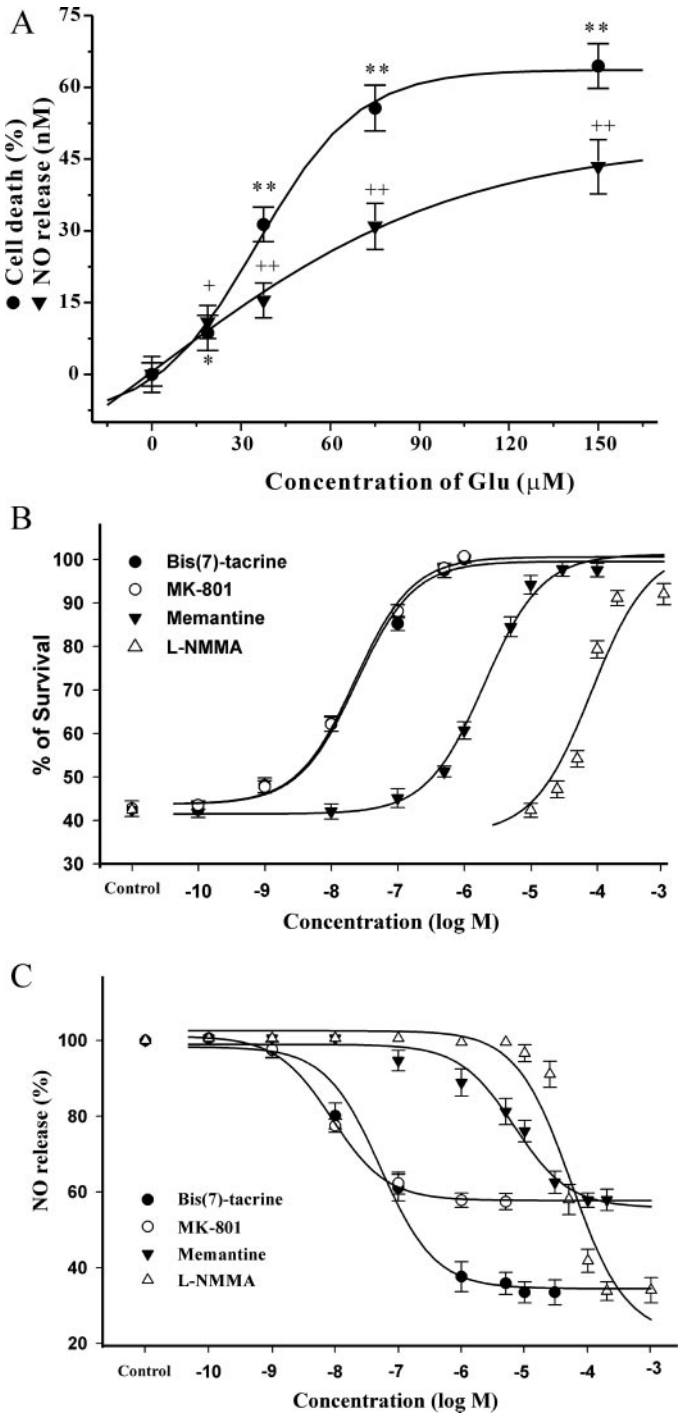

Fig. 1. Bis(7)-tacrine prevents glutamate-induced excitotoxicity and NO release more potently than do memantine and L-NMMA. A, correlation between glutamate-induced excitotoxicity and NO release. For detecting the excitotoxicity of glutamate, at 8 DIV, CGNs were exposed to glutamate at the concentrations indicated. At 24 h after the challenges, the cell viability was measured by MTT assay. All of the data, expressed as the rates of cell death (100 − the percentage of control), are the means ± S.E.M. of three separate experiments; *, $p < 0.05$; **, $p < 0.01$ versus control (ANOVA and Dunnett's test). For detecting the NO release by glutamate, CGNs were exposed to glutamate at the concentrations indicated, and NO concentrations were assayed by the electrochemical method simultaneously. The data were calculated as described under *Materials and Methods*; +, $p < 0.05$; ++, $p < 0.01$ versus control (ANOVA and Dunnett's test). B, bis(7)-tacrine prevents glutamate-induced excitotoxicity more potently than do memantine and L-NMMA. At 8 DIV, CGNs were pretreated with bis(7)-tacrine (0.1 nM to 1 μM)/MK-801 (0.1 nM to 1 μM)/memantine (10 nM to 50 μM)/L-NMMA (10–200 μM) for 2 h before the addition of glutamate (75 μM). The cell viability was measured at 24 h after glutamate challenge. All of the data, expressed as percentages of the corresponding control, are the means ± S.E.M. of three separate experiments. C, bis(7)-tacrine prevents glutamate-induced NO release more potently than do memantine and L-NMMA. At 8 DIV, CGNs were pretreated with bis(7)-tacrine/MK-801/memantine/L-NMMA at the above indicated concentrations for 2 h before the addition of glutamate (75 μM). NO concentrations were measured by the electrochemical method.

that L-NMMA inhibited the release of NO and the cell death caused by glutamate in a concentration-dependent manner (Fig. 1, B and C). Furthermore, we also observed earlier that both L-NMMA at 100 μM and carboxy-2-phenyl-4,4,5,5-tetramethyl-imidazoline-1-oxyl-3-oxide (an NO scavenger) at 10 μM significantly prevent glutamate-induced excitotoxicity in primary cultured cortical neurons (Li et al., 2006).

Bis(7)-tacrine Prevents Glutamate-Induced Excitotoxicity and NO Release More Potently than Do Memantine and L-NMMA. As shown in Fig. 1B, CGNs were pretreated with bis(7)-tacrine (0.1 nM to 1 μM), MK-801 (0.1 nM to 1 μM), memantine (10 nM to 50 μM), and L-NMMA (10–200 μM) for 2 h and then exposed to 75 μM glutamate for 24 h. It was found that bis(7)-tacrine, MK-801, memantine, and L-NMMA prevented glutamate-induced cell death in a concentration-dependent manner with EC_{50} values of 0.024, 0.023, 2.0, and 81.7 μM, respectively. Furthermore, we also found that the selective nNOS inhibitors 7-NI and L-thiocitrulline prevented glutamate-induced cell death with EC_{50} values of 14.7 and 5.9 μM, respectively. We also compared the effects of MK-801, memantine, L-NMMA, and bis(7)-tacrine on the NO release triggered by glutamate using electrochemical methods. As shown in Fig. 1C, bis(7)-tacrine, MK-801, memantine, and L-NMMA reduced the NO release triggered by 75 μM glutamate in a concentration-dependent manner with IC_{50} values of 0.052, 0.012, 6.8, and 54.6 μM, respectively. Similar to L-NMMA, bis(7)-tacrine had higher efficacy than MK-801 and memantine in reducing NO release triggered by glutamate (Fig. 1C).

Bis(7)-tacrine Prevents the Excitotoxicity and NO Release Caused by Glutamate in a Time-Dependent Manner. Compared with 50 μM L-NMMA/5 μM memantine/0.1 μM MK-801, at various pretreatment and concurrent durations, 0.1 μM bis(7)-tacrine significantly prevented the death of CGNs induced by glutamate and still showed significant neuroprotective effects even when added at 1 h after the glutamate insult (strip bar in Fig. 2A), but the potency of its neuroprotective effects significantly decreased with gradually reduced treatment times ($p < 0.01$ between different pretreatment, concurrent, or post-treatment times, ANOVA and Dunnett's test) and completely had no effect when added at 2 h after the glutamate insult. The time course fashion of bis(7)-tacrine, similar to that of L-NMMA, was different from that of MK-801 and memantine in preventing the excitotoxicity caused by glutamate ($p > 0.05$ between different pretreatment times, ANOVA, and Dunnett's test), and we also found that MK-801 and memantine lost their neuroprotective effects when added 1 h after the glutamate challenge (strip bar in Fig. 2A). Similar to their neuroprotection abilities, the effects of bis(7)-tacrine and L-NMMA at various pretreatment and concurrent treatment times ($p < 0.01$ between different pretreatment or concurrent treatment times, ANOVA and Dunnett's test) were different from those of

MK-801 and memantine ($p > 0.05$ between different pretreatment times, ANOVA and Dunnett's test) in reducing the NO release triggered by 75 μM glutamate (Fig. 2B).

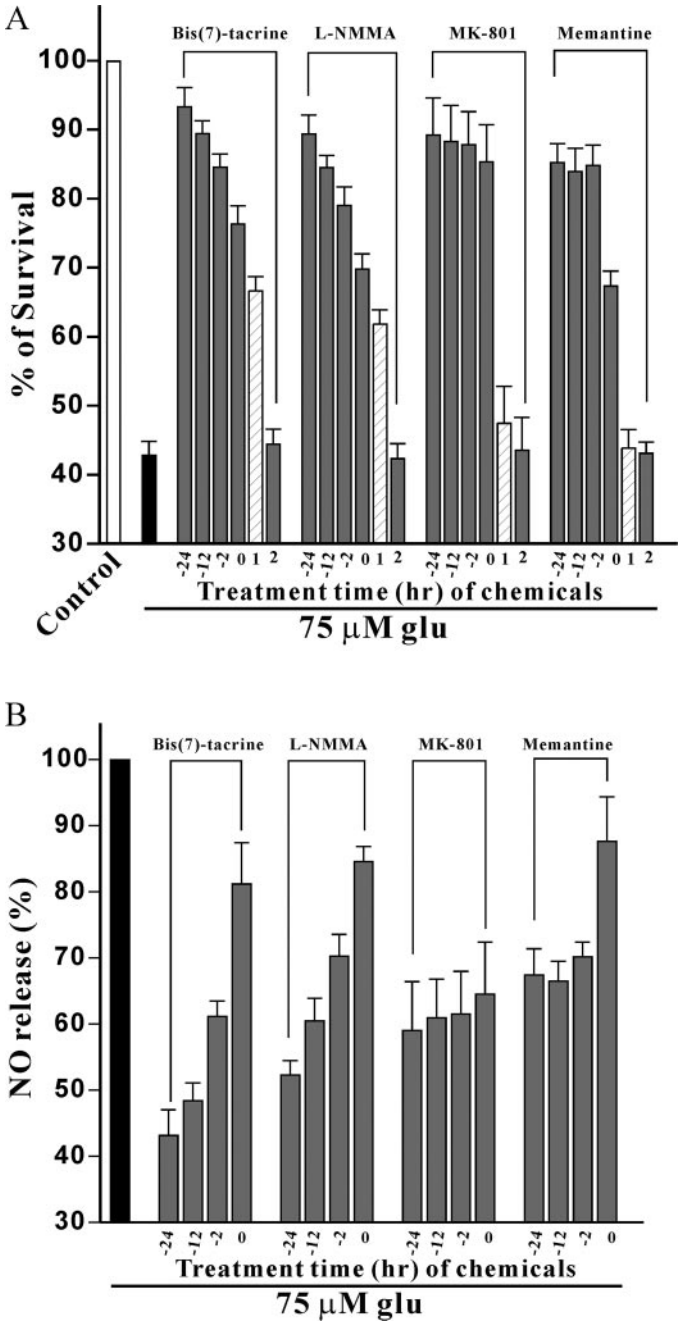

Fig. 2. The time-dependent potency profile of bis(7)-tacrine preventing the excitotoxicity and NO release caused by glutamate. A, bis(7)-tacrine prevents the excitotoxicity in a time-dependent manner. CGNs were exposed to 0.1 μM bis(7)-tacrine/0.1 μM MK-801/5 μM memantine/100 μM L-NMMA 24, 12, and 2 h before glutamate at 75 μM (-24, -12 and -2 h) at the same time as glutamate (0) or 1 and 2 h after glutamate (1 and 2 h). At 24 h after the glutamate challenge, the cell viability was measured by MTT assay. All of the data, expressed as percentages of the corresponding control, are the means ± S.E.M. of three separate experiments. B, bis(7)-tacrine prevents NO release in a time-dependent manner. CGNs were exposed to 0.1 μM bis(7)-tacrine/0.1 μM MK-801/5 μM memantine/100 μM L-NMMA 24, 12, or 2 h before glutamate at 75 μM (-24, -12, or -2 h) or at the same time as glutamate (0). The NO release was detected, and the data were calculated as described under *Materials and Methods*.

Bis(7)-tacrine Blocks NMDAR Moderately. In primary cultured hippocampus neurons at 12 DIV, whole-cell currents were recorded at 100 μM NMDA alone or with the tested drugs. It was found that bis(7)-tacrine, similar to memantine but weaker than MK-801, inhibited NMDA-evoked inward currents (left column of Table 1 and Supplemental Data S1). According to the ligand-receptor binding assay, the affinity of bis(7)-tacrine consistently competed with [^{3}H]MK-801 in rat cerebellar cortical membranes similar to that of memantine but much weaker than that of MK-801 (middle column of Table 1). Furthermore, in CGNs at 8 DIV, glutamate at 50 μM increased intracellular Ca^{2+} by 2.5 times the basal level; and at 1 μM concentrations of the tested drugs, bis(7)-tacrine, close to memantine but weaker than MK-801, significantly reduced the increase of intracellular Ca^{2+} triggered by glutamate (right column of Table 1). However, NOS inhibitors L-NMMA and 7-NI at neuroprotective concentrations failed to inhibit the NMDA-evoked currents in the neurons, failed to compete with [^{3}H]MK-801 in rat cerebellar cortical membranes, and failed to reduce the increase of intracellular Ca^{2+} triggered by glutamate in CGNs (Table 1), which indicated that L-NMMA and 7-NI did not directly interfere with the NMDAR.

Bis(7)-tacrine Inhibits NOS in Vivo and in Vitro. In the NOS activity assays in CGNs, when each of tested drugs was set at 1 μM, we found that bis(7)-tacrine, similar to L-NMMA, slightly inhibited the basal activity of endogenous NOS in CGNs, although its potency was higher than the potency of memantine (left column of Table 2). However, in inhibiting the activity of NOS activated by 75 μM glutamate in CGNs, based on the IC_{50} values, bis(7)-tacrine was approximately 1453 and 250 times more potent than L-NMMA and memantine, respectively (right column of Table 2). In an in vitro NOS activity assay, bis(7)-tacrine was further found to be both direct and more selective in inhibiting recombinant human nNOS over iNOS rather than the eNOS. However, MK-801 and memantine did not inhibit any of the isozymes even at 1 mM. Furthermore, bis(7)-tacrine possessed higher selectivity to nNOS/iNOS over eNOS than 7-NI and L-NMMA in vitro (Table 3).

TABLE 1

Bis(7)-tacrine moderately blocks NMDA receptors

Whole-cell currents were recorded from NMDA (100 μM) alone or NMDA with bis(7)-tacrine/memantine/MK-801/l-NMMA/7-NI at the serial concentrations on primary cultured hippocampal neurons as described under *Materials and Methods*. The IC_{50} values of these chemicals for inhibiting NMDA-evoked currents were calculated by Sigma Plot 9.0 according to the corresponding concentration-response curves. The membrane proteins from rat cerebellar cortex were incubated with [^{3}H]MK-801 (4 nM) as described under *Materials and Methods*. The K_i values were calculated from the corresponding IC_{50} values, which were measured from data obtained using at least eight concentrations of each chemical (in duplicates), based on the Cheng-Prusoff equation: $K_i = IC_{50}/(1 + [\text{ligand}]/K_d)$. The intracellular calcium was detected by confocal microscopy with Fluo-3 dye. The data are expressed as F/F_0, with F representing the fluorescence value after exposure to 50 μM glutamate for 10 min with the indicated chemical, and F_0 representing the fluorescence value just before exposure to glutamate; $n = 30$ for each group.

	NMDA Current, IC_{50}	[^{3}H]MK-801 Binding, K_i	Ca^{2+} influx, F/F_0
	μM	μM	
Control			2.5 ± 0.27
Bis(7)-tacrine	2.5 ± 0.53	0.7 ± 0.045	1.7 ± 0.14
Memantine	3.7 ± 0.69	0.8 ± 0.055	1.9 ± 0.17
MK-801	0.05 ± 0.017	0.04 ± 0.024	1.1 ± 0.13
L-NMMA		N.D.	
7-NI		N.D.	

N.D., not detectable, which indicates that the corresponding chemical has no effect on the tested items.

Bis(7)-tacrine Inhibits nNOS and iNOS in a Competitive Manner. To investigate the patterns of bis(7)-tacrine in nNOS and iNOS inhibition, 1 and 3 μM bis(7)-tacrine were added to the reaction system of nNOS or iNOS reaction systems with L-arginine at concentrations from 5 to 40 μM, respectively. As shown in Fig. 3A, in the Lineweaver-Burk plots, the inhibitory straight lines of bis(7)-tacrine converged on the *y*-axis (V_{max} = 0.041 μmol/mg/min), indicating that bis(7)-tacrine inhibited nNOS by competing with L-arginine. Compared with L-NMMA (K_i = 3.7 μM), bis(7)-tacrine inhibited nNOS with K_i at 1.7 μM (K_m = 6.3 μM L-arginine alone) (Fig. 4B). On the other hand, bis(7)-tacrine also competitively inhibited iNOS with L-arginine, and compared with L-NMMA (K_i = 9.1 μM), bis(7)-tacrine inhibited iNOS with K_i at 5.8 μM (K_m = 8.1 μM L-arginine alone).

Molecular Docking Simulation of the Interaction between Bis(7)-tacrine and NOS Isozymes. To gain further insight into the interaction mechanisms between bis(7)-tacrine and three NOS isoforms, computational docking was performed to dock bis(7)-tacrine separately to nNOS, iNOS, and eNOS. The estimated free energy of bis(7)-tacrine binding to nNOS had the lowest value (−14.93 kcal/mol) compared with those of bis(7)-tacrine binding to iNOS (−14.17 kcal/mol) and eNOS (−13.35 kcal/mol). In the bis(7)-tacrine-nNOS complex, hydrogen bonds were formed at the tacrine moiety with Glu592 and the heme at the bottom of the pocket (Fig. 4A, a), and in the bis(7)-tacrine-iNOS complex, the same type of bonds were formed between the tacrine moiety and the amino acids Glu371 (at the bottom of the pocket), Glu488, and Asn348 (near the top of the pocket) (Fig. 4A, b); a hydrogen bond was only formed between Glu361 and the tacrine moiety in the bis(7)-tacrine-eNOS complex (Fig. 4A, c). Furthermore, there were two characteristics of the interactions between bis(7)-tacrine and NOS iosforms: a glutamate (Glu592 of nNOS, Glu371 of iNOS, and Glu361 of eNOS) located at the pocket bottom formed a hydrogen bond with the nitrogen atom of one tacrine moiety of bis(7)-tacrine (Fig. 4B, a–c), and bis(7)-tacrine formed hydrophobic interactions with nNOS and iNOS at both the bottom and top of the pocket (Fig. 4A, a and b).

Discussion

We have reported that bis(7)-tacrine prevents glutamate-induced neuronal apoptosis in CGNs (Li et al., 2005). In the current study, the model of glutamate-induced excitotoxicity in CGNs was used to investigate further the precise mechanisms underlying the superior neuroprotective activities of bis(7)-tacrine. In CGNs, there is a correlation between the excitotoxicity and NO release caused by glutamate (Fig. 1A), and the NOS inhibitor L-NMMA significantly reduced the NO release and the cell death induced by glutamate (Fig. 1, B and C). Furthermore, both selective nNOS inhibitors (7-NI and L-thiocitrulline) and a NO scavenger [2-(4-carboxyphenyl)-4,4,5,5- tetra-methyl-imidazoline-1-oxyl-3-oxide] significantly prevented glutamate-induced neurotoxicity (Li et al., 2006). Together, these results suggest that NO mediates glutamate-induced excitotoxicity. Because bis(7)-tacrine can significantly reduce glutamate-induced excitotoxicity (Li et al., 2005), we investigated how bis(7)-tacrine affected glutamate-induced NO generation. As shown in Fig. 1, B and C, similar to MK-801, bis(7)-tacrine was approximately 80 and 3400 times more potent in reducing the excitotoxicity and 130 and 1050 times more potent in inhibiting the NO release than were memantine and L-NMMA, respectively. These results indicate that there is a correlation between neuroprotection and the inhibitory ability of NO formation by bis(7)-tacrine.

How did bis(7)-tacrine inhibit the NO release induced by glutamate at such high potency? Endogenous NO is produced only by NOS when L-arginine is converted into L-citrulline (Fedorov et al., 2004; Blaise et al., 2005). Therefore, the reduction of NO may be caused by either inhibiting NOS or scavenging NO. Bis(7)-tacrine fails to inhibit the cell death and the NO release induced by an NO donor, sodium nitroprusside (Li et al., 2006), indicating that the inhibition of NO generated by NOS may contribute to the neuroprotection of bis(7)-tacrine instead of scavenging NO. Excessive glutamate may overactivate NOS through overloading intracellular Ca^{2+} and/or altering the conformation of the postsynaptic density protein-95-NMDAR coupling protein; and the blockade of NMDAR or the interference of this coupling protein may inhibit the activation of NOS caused by glutamate (Sattler et al., 1999; Aarts et al., 2002). However, bis(7)-tacrine failed to interfere with their interaction (data not shown), suggesting that the NO inhibition is likely to be via an NMDAR blockade. Our results indeed suggested that bis(7)-tacrine, similarly to memantine but much more weakly than MK-801, blocks NMDAR at the MK-801 site and then reduces the glutamate-triggered increase of intracellular Ca^{2+}

TABLE 2

Differential inhibition of basal and overactivated nNOS by bis(7)-tacrine

The activity of NOS and its inhibition by different chemicals were measured in CGNs by the NOS assay kit as described under *Materials and Methods*. Relative inhibitory potency was expressed as [1 − (NOS activity of group with the drug at 1 μM over that of control group)] × 100%. The IC_{50} value of each chemical to inhibit endogenous NOS in CGNs treated with glutamate at 75 μM was obtained from eight-point titration using Sigma Plot 9.0, where each individual point was an average of duplicate determination at the same concentration from three independent experiments. Glutamate at 75 μM increased the activity of NOS by 2.7 ± 0.37-fold of the basal level.

Drug	Basal NOS (without Glutamate), Relative Inhibitory Potency at 1 μM	Activated NOS (with Glutamate) IC_{50}
	%	μM
Bis(7)-tacrine	4.5 ± 0.36	0.03 ± 0.0061
L-NMMA	3.7 ± 0.45	43.6 ± 5.73
Memantine	0.8 ± 0.29	7.5 ± 0.96

TABLE 3

Selective inhibition of nNOS by bis(7)-tacrine in vitro

In vitro, the activity of the recombinant human nNOS, eNOS, and iNOS and their inhibition by chemicals were measured by the NOS assay kit as described under *Materials and Methods*. The IC_{50} value of each chemical to inhibit nNOS, iNOS, and eNOS was obtained from eight-point titration using Sigma Plot 9.0, where each individual point was an average of duplicate determination at the same concentration from three independent experiments.

Drug	IC_{50}		
	nNOS	iNOS	eNOS
		μM	
Bis(7)-tacrine	2.9 ± 0.21	9.3 ± 0.59	>100
L-NMMA	4.1 ± 0.17	15.0 ± 0.37	3.8 ± 0.41
7-NI	0.7 ± 0.19	27.7 ± 0.76	1.9 ± 0.35
MK-801		N.D.	
Memantine		N.D.	

N.D., not detectable, which indicates that the corresponding chemical does not inhibit the activity of NOS even at 1 mM.

(Table 1), which may contribute to the inhibition of NO production via indirectly inhibiting NOS. However, how do we explain the discrepancy between the moderate blockade of NMDAR and the high neuroprotection potency by bis(7)-tacrine?

Bis(7)-tacrine and L-NMMA significantly inhibit NO-mediated neuronal cell death caused by glutamate and L-arginine and in cortical neurons (Li et al., 2006), whereas MK-801 cannot prevent neuronal cell death induced by L-arginine (Yamauchi et al., 1998). Under various different treatment durations, the time-dependent potency of bis(7)-tacrine, similar to that of L-NMMA, was different from that of MK-801 and memantine in reducing cell death and NO release. Moreover, bis(7)-tacrine and L-NMMA still possessed significant neuroprotective effects even when added 1 h after glutamate challenge (Fig. 2). Together, these findings suggest that besides blocking NMDAR, bis(7)-tacrine may have intracellular targets for NOS inhibition. Therefore, we hypothesized that bis(7)-tacrine might directly inhibit the activity of NOS in this study. In live neurons, bis(7)-tacrine showed significant neuroprotection effects at low concentrations (such as 1 nM; Fig. 1B), which is matched with its high inhibitory potency for glutamate-induced NO release and NOS activation. In vitro, bis(7)-tacrine directly inhibited the activity of purified NOS with higher selectivity toward nNOS and iNOS (Table 3). Furthermore, bis(7)-tacrine did not alter V_{max} but increased the observed K_m (Fig. 3A), and the observed K_m and corresponding concentration of bis(7)-tacrine had a linear relationship (Fig. 3B). Our results suggest that bis(7)-tacrine directly inhibits nNOS and iNOS in a competitive way with L-arginine.

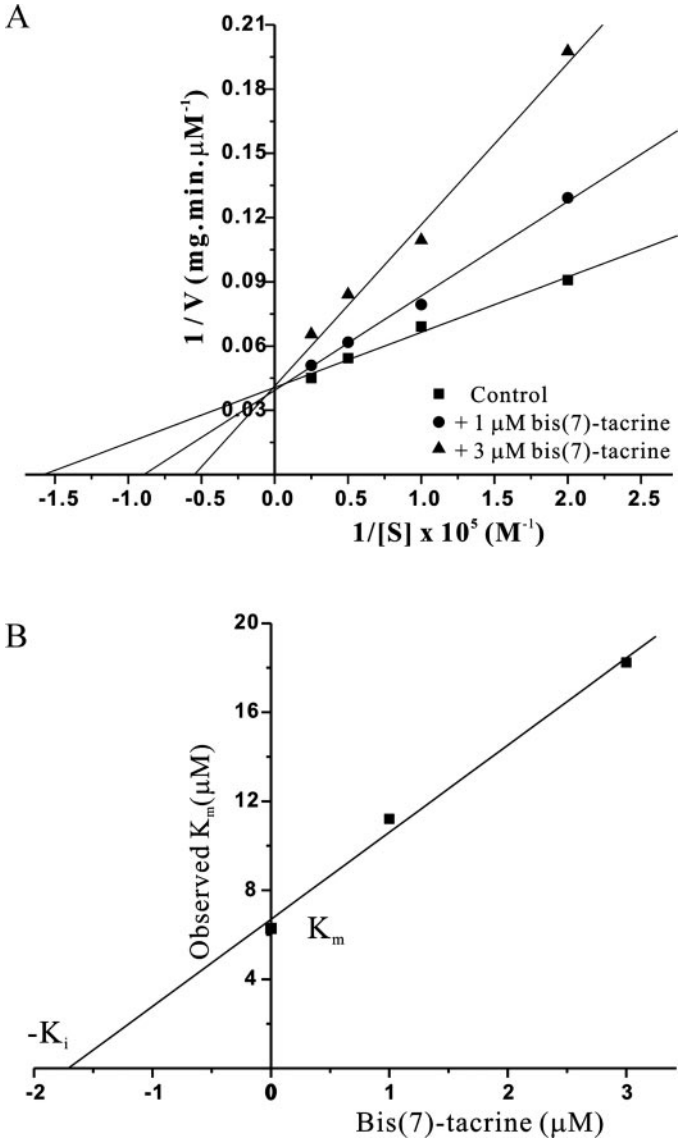

Fig. 3. Selective inhibition of nNOS by bis(7)-tacrine in a competitive manner. A, pattern analysis of nNOS inhibition with L-arginine by bis(7)-tacrine. Recombinant nNOS (2.5 μg) was assayed in either the presence (1 or 3 μM) or absence of bis(7)-tacrine under the conditions with 5 to 40 μM L-[^{3}H]arginine. The plots of $1/V$ versus $1/[S]$ were fitted by a Lineweaver-Burk straight-line with an intercept of $1/V_{max}$ and a slope of K_m/V_{max}. The data are expressed as the means from three independent experiments. B, the K_i value of bis(7)-tacrine to inhibit nNOS. The plot of the observed K_m values from A versus concentrations of bis(7)-tacrine was drawn by the linear fit.

By using the docking-simulation technique, we investigated the molecular interaction mechanisms between bis(7)-tacrine and three NOS isozymes. In the bis(7)-tacrine-nNOS complex, the tacrine moiety closely contacted with Tyr706 (Fig. 4A, a). The hydrophobic interaction between bis(7)-tacrine and Tyr706 facilitated a long inhibition with nNOS. Because bis(7)-tacrine is also a bivalent inhibitor of AChE (Pang et al., 1996), aromatic residues such as Trp279 and Tyr70 that are located at the peripheral site of the AChE gorge can also form hydrophobic interactions with any bivalent AChE inhibitors such as donpezil, which control the bivalent inhibitors entering or leaving the gorge (Kryger et al., 1999; Niu et al., 2005). Therefore, we conclude that the aromatic residue of Tyr706 also plays an important role in controlling the bis(7)-tacrine binding in nNOS. In the bis(7)-tacrine-iNOS complex, although bis(7)-tacrine formed hydrogen bonds with Asn348 and Glu488, the affinity of bis(7)-tacrine to iNOS was actually lower than that with nNOS, which may be due to the further distance between the bis(7)-tacrine and Y485 (Fig. 4A, b). In the bis(7)-tacrine-eNOS complex, bis(7)-tacrine only formed hydrophobic interactions with Trp447 at the top of the pocket (Fig. 4A, c), which therefore causes the lowest affinity of bis(7)-tacrine to eNOS among the three NOS isoforms.

NO and glutamate are important bioregulatory molecules in various organs for daily activities of cells. It is only at elevated concentrations that NO and glutamate are involved in cytotoxic events (Aarts et al., 2002; Drummond et al., 2005). Therefore, it is of great significance to find drugs that inhibit the overactivation of NMDAR and NOS instead of interfering with NO and glutamate's normal physiological functions. Moderate affinity antagonists of NMDAR, such as memantine, actually have high success in the treatment of numerous central nervous system disorders because drugs with this property may prevent glutamate excitotoxicity without producing undesirable side effects within the therapeutic dosages, whereas high-affinity antagonists such as MK-801 may produce severe adverse effects (Danysz and Parsons, 2003; Li et al., 2005). It is very interesting that bis(7)-tacrine has a moderate affinity to NMDAR (Table 1). Furthermore, bis(7)-tacrine has been shown to cross the blood-brain barrier easily (Wang et al., 1999) with no significant side effect at the proposed therapeutic dosages (Liu et al., 2000). On the other hand, bis(7)-tacrine at 1 μM nearly completely prevents glutamate-induced cell death but only

slightly inhibits the basal activity of NOS in CGNs (Table 2), indicating that, at effective concentrations, this compound may not interfere with the normal physiological functions of NO. Even though L-NMMA at 1 μM also slightly inhibited NOS basal activity, it exhibited significant neuroprotective effects only at high concentrations (more than 50 μM; Fig. 1B), which is matched with its relatively lower ability in reducing the glutamate-induced NOS activation (Table 2). It can be rationally proposed that L-NMMA at effective neuroprotective concentrations may also strongly inhibit the activity of physiological NOS and the normal functioning of NO. Furthermore, bis(7)-tacrine possesses higher selectivity toward nNOS and iNOS than eNOS in vitro. In addition, the activation of iNOS is independent of intracellular Ca^{2+} increases triggered by glutamate (Alderton et al., 2001; Strub et al., 2006). Therefore, bis(7)-tacrine at neuroprotective concentrations may inhibit the activity of nNOS overactivated by glutamate without interfering with eNOS and iNOS. It is very encouraging that synergistic neuroprotective effects have been shown by combining an NMDA receptor antagonist with NOS inhibitors in the treatment of cerebral ischemia (Hicks et al., 1999). In our system, we found that 0.1 μM memantine combined with 10 μM L-NMMA or with 10 μM 7-NI were much more potent than each chemical alone in reducing the excitotoxicity caused by glutamate (Fig. 5A), suggesting that the concurrent blockage of NMDAR and NOS may be synergistically neuroprotective against the excitotoxicity.

In summary, bis(7)-tacrine prevents glutamate-induced excitotoxicity by the reduction of excessive NO release through inhibiting nNOS in both direct (i.e., inhibition of nNOS) and indirect (i.e., moderately blocking NMDAR,

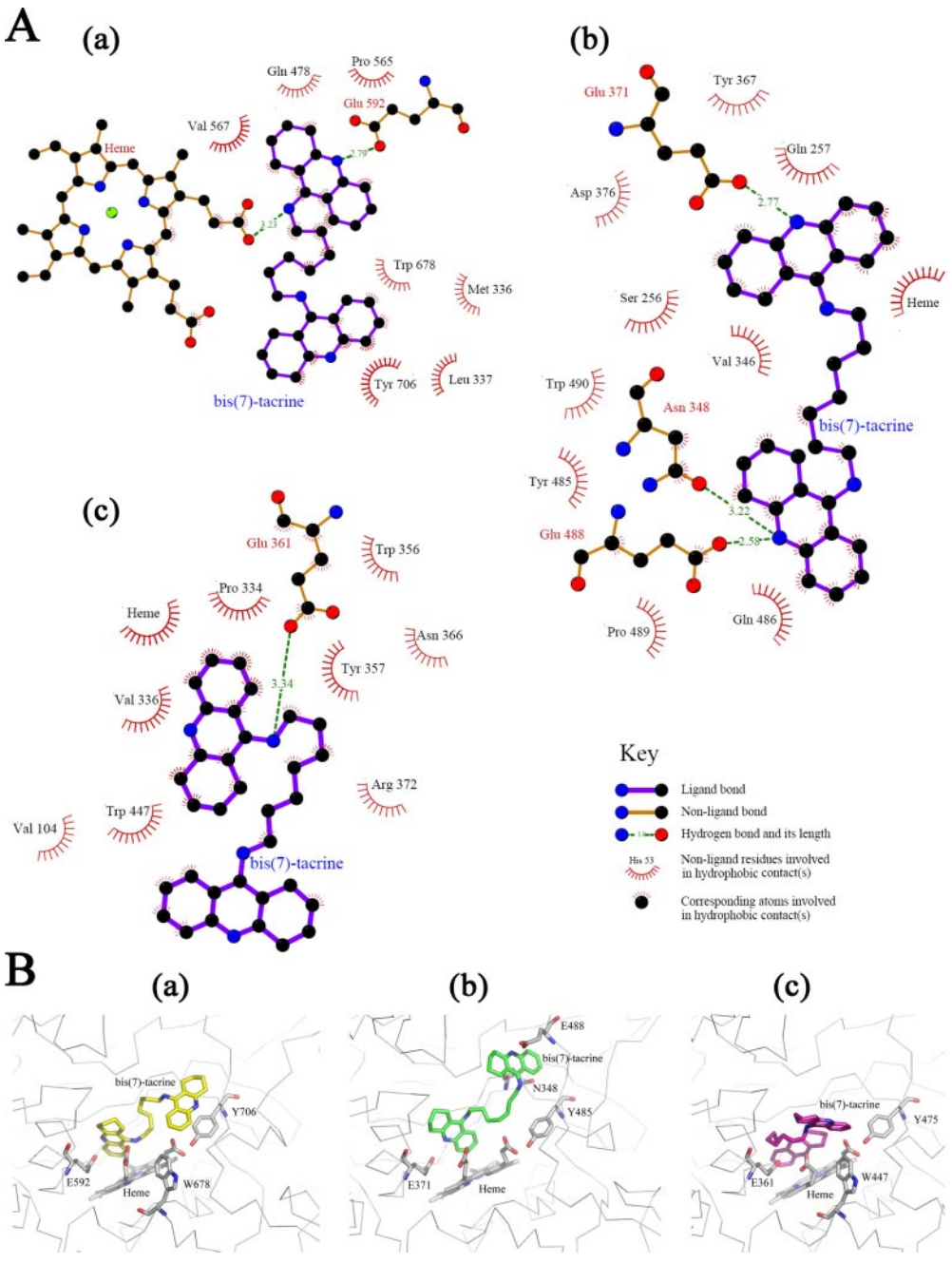

Fig. 4. Molecular docking simulation of selective interactions between bis(7)-tacrine and nNOS. A, schematic representation of hydrogen bonds and hydrophobic interactions between bis(7)-tacrine and nNOS (a), iNOS (b), and eNOS (c). The broken lines represent the hydrogen bonds, and spiked resides form the hydrophobic interactions with bis(7)-tacrine. This figure was made with the LIGPLOT program. B, the patterns of selective interactions between bis(7)-tacrine and nNOS (a), iNOS (b), and eNOS (c). The figures were prepared using the PYMOL program.

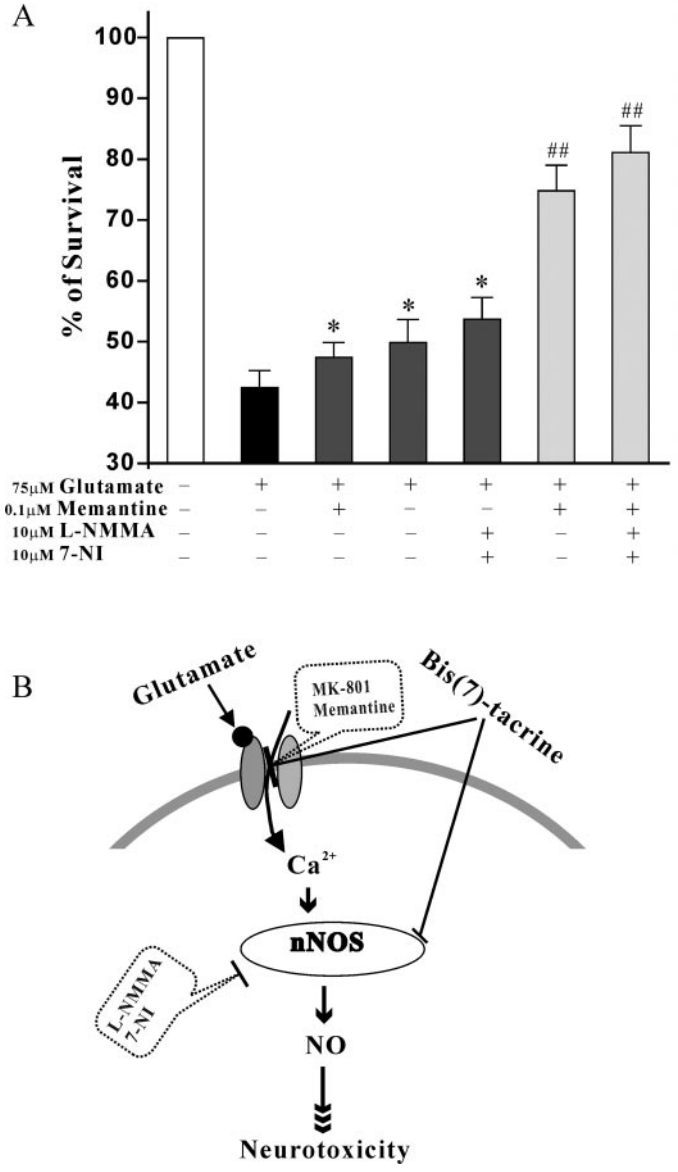

Fig. 5. Concurrent blockage of NMDAR and nNOS shows the proposed dual mechanism of synergistic neuroprotection against glutamate. A, synergistic protection against glutamate-induced excitotoxicity by combination of memantine and L-NMMA or 7-NI. At 8 DIV, CGNs were exposed to 0.1 μM memantine/10 μM L-NMMA/10 μM 7-NI/(0.1 μM memantine + 10 μM L-NMMA)/(0.1 μM memantine + 10 μM 7-NI) for 2 h before glutamate at 75 μM. At 24 h after the glutamate challenge, the cell viability was measured by MTT assay. All of the data, expressed as percentages of the corresponding control, are the means ± S.E.M. of three separate experiments; *, $p < 0.05$ versus glutamate alone group; ##, $p < 0.01$ versus memantine, L-NMMA, or 7-NI alone (ANOVA and Dunnett's test). B, the proposed dual mechanism of synergistic neuroprotection against glutamate by bis(7)-tacrine. When neurons are exposed to glutamate at toxic concentrations, excessive NO mediates NMDAR downstream-signaling pathways that trigger excitotoxicity. Bis(7)-tacrine concurrently blocks NMDAR and inhibits nNOS, thereby synergistically providing substantial neuroprotection.

which reduces the influx of Ca^{2+} and inhibits NOS activation) mechanisms, which are synergistically neuroprotective (Fig. 5B). Although further studies are needed to rule out other possible targets, here we can conclude that at least the concurrent blockade of NMDAR and neuronal NOS is involved in the mechanisms underlying neuroprotection by bis(7)-tacrine. This conclusion may explain why bis(7)-tacrine has higher potency than memantine or L-NMMA in reducing glutamate-induced excitotoxicity, although it possesses similar potency to block NMDA receptors as does memantine, or to inhibit nNOS as does L-NMMA in vitro. Our findings here strongly suggest that the novel AChE inhibitor bis(7)-tacrine is also a moderate NMDAR antagonist and a selective nNOS inhibitor. Given burgeoning and increasing evidence suggesting that multifunctional compounds might provide greater therapeutic efficacy for neurodegenerative diseases by concurrently targeting different sites in the brain (Youdim and Buccafusco, 2005), these and our results published previously lead us to conjecture that the multipotencies of bis(7)-tacrine may synergistically contribute to reducing the effects of various neurodegenerative disorders which may offer a novel direction for rational development of new agents for the prevention and treatment of neurodegenerative diseases.

Acknowledgments

We sincerely thank Professor Donald C. Chang for kindly providing the confocal laser scanning microscopy for the intracellular calcium assay and Dr. Virginia Anne Unkefer for carefully editing and proofreading our manuscript.

References

Aarts M, Liu Y, Liu L, Besshoh S, Arundine M, Gurd JW, Wang YT, Salter MW, and Tymianski M (2002) Treatment of ischemic brain damage by perturbing NMDA receptor- PSD-95 protein interactions. *Science (Wash DC)* **298:**846–850.

Alderton WK, Cooper CE, and Knowles RG (2001) Nitric oxide synthases: structure, function and inhibition. *Biochem J* **357:**593–615.

Berman HM, Westbrook J, Feng Z, Gilliland G, and Bhat TN (2000) The Protein Data Bank. *Nucleic Acids Res* **28:**235–242.

Blaise GA, Gauvin D, Gangal M, and Authier S (2005) Nitric oxide, cell signaling and cell death. *Toxicology* **208:**177–192.

Boje KM (2004) Nitric oxide neurotoxicity in neurodegenerative diseases. *Front Biosci* **9:**763–776.

Danysz W and Parsons CG (2003) The NMDA receptor antagonist memantine as symptomatological and neuroprotective treatment for Alzheimer's disease: preclinical evidence. *Int J Geriatr Psychiatry* 18:S23–S32.

Drummond JC, McKay LD, Cole DJ, and Patel PM (2005) The role of nitric oxide synthase inhibition in the adverse effects of etomidate in the setting of focal cerebral ischemia in rats. *Anesth Analg* **100:**841–846.

Fedorov R, Vasan R, Ghosh DK, and Schlichting I (2004) Structures of nitric oxide synthase isoforms complexed with the inhibitor AR-R17477 suggest a rational basis for specificity and inhibitor design. *Proc Natl Acad Sci USA* **101:**5892–5897.

Fischmann TO, Hruza A, Xiao DN, Fossetta JD, Lunn CA, Dolphin E, Prongay AJ, Reichert P, Lundell DJ, Narula SK, et al. (1999) Structural characterization of nitric oxide synthase isoforms reveals striking active-site conservation. *Nat Struct Biol* **6:**233–242.

Frantz S (2005) Drug discovery: playing dirty. *Nature (Lond)* **437:**942–943.

Fu H, Li W, Lao Y, Luo J, Lee NT, Kan KK, Tsang HW, Tsim KW, Pang Y, Li Z, et al. (2006) Bis(7)-tacrine attenuates beta amyloid-induced neuronal apoptosis by regulating L-type calcium channels. *J Neurochem* **98:**1400–1410.

Grunewald T and Beal MF (1999) NOS knockouts and neuroprotection. *Nat Med* **5:**1354–1355.

Hicks CA, Ward MA, Swettenham JB, and O'Neill MJ (1999) Synergistic neuroprotective effects by combining an NMDA or AMPA receptor antagonist with nitric oxide synthase inhibitors in global cerebral ischaemia. *Eur J Pharmacol* **381:**113–119.

Kryger G, Silman I, and Sussman JL (1999) Structure of acetylcholinesterase complexed with E2020 (Aricept); implications for the design of new anti-Alzheimer drugs. *Structure Fold Des* **7:**297–307.

Li W, Lee NT, Fu H, Kan KK, Pang Y, Li M, Tsim KW, and Han Y (2006) Neuroprotection via inhibition of nitric oxide synthase by bis(7)-tacrine. *Neuroreport* **17:**471–475.

Li W, Pi R, Chan HH, Fu H, Lee NT, Tsang HW, Pu Y, Chang DC, Li C, Luo J, et al. (2005) Novel dimeric acetylcholinesterase inhibitor bis7-tacrine, but not donepezil, prevents glutamate-induced neuronal apoptosis by blocking *N*-methyl-D-aspartate receptors. *J Biol Chem* **280:**18179–18188.

Lipton SA (2004) Paradigm shift in NMDA receptor antagonist drug development: molecular mechanism of uncompetitive inhibition by memantine in the treatment of Alzheimer's disease and other neurologic disorders. *J Alzheimers Dis* **6:**S61–S74.

Liu J, Ho W, Lee NT, Carlier PR, Pang Y, and Han Y (2000) Bis(7)-tacrine, a novel acetylcholinesterase inhibitor, reverses AF64A-induced deficits in navigational memory in rats. *Neurosci Lett* **282:**165–168.

Mattson MP (2004) Pathways towards and away from Alzheimer's disease. *Nature (Lond)* **430:**631–639.

Morris GM, Goodsell DS, Halliday RS, Huey R, Hart WE, Belew RK, and Olson AJ

(1998) Automated docking using a Lamarckian genetic algorithm and an empirical binding free energy function. *J Comput Chem* **19:**1639–1662.
Niu CY, Xu YC, Xu Y, Luo XM, Duan WH, Silman I, Sussman JL, Zhu WL, Chen KX, Shen JH, et al. (2005) Dynamic mechanism of E2020 binding to acetylcholinesterase: a steered molecular dynamics simulation. *J Phys Chem B* **109:**23730–23738.
Pang YP, Quiram P, Jelacic T, Hong F, and Brimijoin S (1996) Highly potent, selective, and low cost bis-tetrahydroaminacrine inhibitors of acetylcholinesterase. Steps toward novel drugs for treating Alzheimer's disease. *J Biol Chem* **271:**23646–23649.
Sattler R, Xiong Z, Lu WY, Hafner M, MacDonald JF, and Tymianski M (1999) Specific coupling of NMDA receptor activation to nitric oxide neurotoxicity by PSD-95 protein. *Science (Wash DC)* **284:**1845–1848.
Sonkusare SK, Kaul CL, and Ramarao P (2005) Dementia of Alzheimer's disease and other neurodegenerative disorders—memantine, a new hope. *Pharmacol Res* **51:**1–17.
Strijbos PJ, Leach MJ, and Garthwaite J (1996) Vicious cycle involving Na+ channels, glutamate release, and NMDA receptors mediates delayed neurodegeneration through nitric oxide formation. *J Neurosci* **16:**5004–5013.
Strub A, Ulrich WR, Hesslinger C, Eltze M, Fuchss T, Strassner J, Strand S, Lehner MD, and Boer R (2006) The novel imidazopyridine 2-[2-(4-methoxy-pyridin-2-yl)-ethyl]-3H-imidazo [4,5-b] pyridine (BYK191023) is a highly selective inhibitor of the inducible nitric-oxide synthase. *Mol Pharmacol* **69:**328–337.
Van der Schyf CJ, Geldenhuys WJ, and Youdim MB (2006) Multifunctional drugs with different CNS targets for neuropsychiatric disorders. *J Neurochem* **99:**1033–1048.
Wang H, Carlier PR, Ho WL, Wu DC, Lee NT, Li CP, Pang YP, and Han YF (1999) Effects of bis(7)-tacrine, a novel anti-Alzheimer's agent, on rat brain AChE. *Neuroreport* **10:**789–793.
Willmot M, Gibson C, Gray L, Murphy S, and Bath P (2005) Nitric oxide synthase inhibitors in experimental ischemic stroke and their effects on infarct size and cerebral blood flow: a systematic review. *Free Radic Biol Med* **39:**412–425.
Wu DC, Xiao XQ, Ng AK, Chen PM, Chung W, Lee NT, Carlier PR, Pang YP, Yu AC, and Han YF (2000) Protection against ischemic injury in primary cultured mouse astrocytes by bis(7)-tacrine, a novel acetylcholinesterase inhibitor. *Neurosci Lett* **288:**95–98.
Xiao XQ, Lee NT, Carlier PR, Pang Y, and Han YF (2000) Bis(7)-tacrine, a promising anti-Alzheimer's agent, reduces hydrogen peroxide-induced injury in rat pheochromocytoma cells: comparison with tacrine. *Neurosci Lett* **290:**197–200.
Xue J, Ying X, Chen J, Xian Y, and Jin L (2000) Amperometric ultramicrosensors for peroxynitrite detection and its application toward single myocardial cells. *Anal Chem* **72:**5313–5321.
Yamauchi M, Omote K, and Ninomiya T (1998) Direct evidence for the role of nitric oxide on the glutamate-induced neuronal death in cultured cortical neurons. *Brain Res* **780:**253–259.
Youdim MB and Buccafusco JJ (2005) Multi-functional drugs for various CNS targets in the treatment of neurodegenerative disorders. *Trends Pharmacol Sci* **26:**27–35.
Yuan J and Yankner BA (2000) Apoptosis in the nervous system. *Nature (Lond)* **407:**802–809.
Zhang HY (2005) One-compound-multiple-targets strategy to combat Alzheimer's disease. *FEBS Lett* **579:**5260–5264.

Address correspondence to: Dr. Yifan Han, Department of Biochemistry, Hong Kong University of Science and Technology, Clear Water Bay, Kowloon, Hong Kong SAR, China. E-mail: bcyfhan@ust.hk